Pressure Effects on the Photocycle of Purple Membrane†

Jeffrey Marque and Laura Eisenstein*

ABSTRACT: We studied the effects of hydrostatic pressure on the kinetics of the photocycle of purple membrane from *Halobacterium halobium*. The data were interpreted in terms of a unidirectional and unbranched model. We found that all of the distinct processes of the photocycle are retarded by pressure, with the earlier, fast processes showing less sensitivity to pressure than the later, slow processes. The qualitative similarity of these results with the effects of solvent viscosity on the photocycle kinetics suggests that the primary effects of pressure on the kinetics are via the intrinsic viscosity of the membrane and not via activation volumes. There is a strong quantitative correlation between the pressure effects and the solvent viscosity effects, further supporting this interpretation. We observed a monotonic decrease in the positive absorbance change signal at 640 nm near the end of the photocycle as the pressure is increased. This signal is usually ascribed to the O intermediate, and we interpreted our finding, along with evidence from other experiments, to mean that an ionizable group or groups, such as carboxylic acids, are undissociated and uncharged in O.

Purple membrane is the light-driven proton pump found in the cell membrane of *Halobacterium halobium*. Purple membrane contains a single protein, bacteriorhodopsin (bR).[1] The chromophore in bR is a molecule of retinal covalently bound to a lysine residue (Lys-216) via a protonated Schiff base linkage. Purple membrane functions by absorbing visible radiation and using the energy to pump protons from the inside to the outside of the bacterial cell, thus generating a transmembrane electrochemical gradient. The bacterium is able to couple the relaxation of the gradient, elsewhere on the cell membrane, to the phosphorylation of adenosine 5′-diphosphate. Purple membrane thus enables the bacterium to generate adenosine 5′-triphosphate (ATP) in the absence of oxygen and thereby survive in anaerobic environments.

Associated with the movement of protons across the purple membrane are complicated color changes in the purple membrane. These color changes are collectively referred to as the purple membrane photocycle, or bacteriorhodopsin photocycle (Lozier et al., 1975). The photocycle is not a well-defined concept; different workers have different opinions as to the number of intermediates and to the reactions between those intermediates. In the literature, one finds an entire gamut of phenomenological models for the photocycle, from the simple sequential model, bR $\rightsquigarrow$ K $\rightarrow$ L $\rightarrow$ M $\rightarrow$ O $\rightarrow$ bR, to much more complicated and multibranched models. For further details concerning the structure of purple membrane and the nature of the photocycle, the reader is referred to any of the several review articles (Henderson, 1977; Stoeckenius et al., 1979; Ottolenghi, 1980; Birge, 1981; Stoeckenius & Bogomolni, 1982).

In this paper, we report the effects of hydrostatic pressure on the kinetics of the photocycle. In spite of our knowledge that the simple sequential model sketched above probably does not completely describe that photocycle, we have chosen to use it as an approximation of the photocycle because it contains the essential features that are contained in our data.

In an effort to understand the molecular basis for the proton pump, workers have studied the effects of a variety of environmental factors on the photocycle. Nagle et al. (1982) probably have the most complete data sets that probe the effect of temperature on the photocycle. Govindjee et al. (1980) and Sherman et al. (1976) have studied the effects of ionic strength, and Ort & Parson (1978) have studied the effects of pH on the kinetics of the photocycle. We have studied the effects of solvent viscosity on the photocycle kinetics (Beece et al., 1981) and were able to measure the effects of the solvent viscosity on four processes within the photocycle.

An important finding from our study is that solvent viscosity profoundly affects the last slow steps of the photocycle. In our analysis, we were able to separate the effects of temperature on the solvent and on the membrane. This separation was accomplished by modeling the kinetics via a modified Kramers' equation (Kramers, 1940; Beece et al., 1980):

$$k = (A/\eta^{\kappa})e^{-\Delta H^{\ddagger}/(k_B T)} \quad (1)$$

where η is the solvent viscosity, k_B is the Boltzmann constant, and T is the absolute temperature. We also analyzed our data in terms of the more traditional Arrhenius expression:

$$k = A'e^{-\Delta H'^{\ddagger}/(k_B T)} \quad (2)$$

As can be seen in the results of our viscosity paper (Beece et al., 1981), the effect of using a modified Kramers' equation is not just to explicitly account for the solvent viscosity in describing the photocycle dynamics. Another effect is to derive activation enthalpies ($\Delta H^{\ddagger}$) that more accurately describe the reaction site than can be derived from an Arrhenius plot. Specifically, we found that the use of Arrhenius plots gave erroneously high activation enthalpies ($\Delta H'^{\ddagger}$) because such plots lump two independent effects together: (1) the increase in the rate with increasing temperature due to an activation enthalpy and (2) the increase in the rate with increasing temperature due to a decrease in the solvent viscosity. The first effect is a local one, due to temperature's modulation of the reactant population that has sufficient energy to go over a local potential barrier. The second effect is nonlocal. It describes the effect of viscous drag by the solvent on the entire bacteriorhodopsin molecule. Because the second effect is a nonlocal one, it is conceptually incorrect to lump it together

† From the Department of Physics, University of Illinois at Urbana-Champaign, Urbana, Illinois 61801. *Received January 10, 1984; revised manuscript received May 31, 1984.* The work was supported in part by Grant GM18051 from the Department of Health and Human Services, USPHS, and by Grants PCM82-09616 and INT82-17661 from the National Science Foundation.

[1] Abbreviations: bR, bacteriorhodopsin; ATP, adenosine 5′-triphosphate.

0006-2960/84/0423-5556$01.50/0

with the effect of the activation enthalpy.

However, we neglected yet another possible nonlocal effect of temperature: the decrease of the intrinsic membrane viscosity due to thermal expansion of the membrane as the temperature is raised. One of the reasons we chose to measure the effects of pressure on the photocycle, therefore, was to see if we could compensate for thermal expansion of the membrane by compressing it and then seeing how much of the temperature effect (on the kinetics) could be attributed to an activation barrier and how much could be attributed to modulation of the membrane viscosity. There is a large body of evidence (Chin et al., 1976; Cossins et al., 1980; Cossins & Prosser, 1982; Chong, 1982; Chong & Cossins, 1983) that suggests the modulation of membrane viscosity by temperature and pressure. We have no methods in our laboratory for measuring membrane viscosity, so this aspect of our study can only be qualitative. As we shall show later in this paper, however, the qualitative results give strong evidence that it is precisely via membrane viscosity that pressure exerts its major effects on photocycle kinetics. Finally, pressure may also give us some clues as to the physical nature of some of the photocycle intermediates, usually referred to as K, L, M, and O.

Materials and Methods

Purple membrane samples were obtained from the laboratory of Professor T. G. Ebrey. They were washed several times in one of six different aqueous buffers. All of the buffers were 10 mM in imidazole, but they had varying amounts of HCl added, according to the temperature at which an experiment was to be performed, so that the six buffers were at pH 7.2 ± 0.1 at 1, 8.6, 24.6, 33.5, 38.4, or 50.0 °C, respectively. (Hereafter, we shall refer to these as 1, 9, 25, 33, 38, and 50 °C, respectively.) Tsuda et al. (1976) have shown that such buffers are pH constant to within better than 0.1 pH unit over the pressure range of 1 atm to 4 kbar.

After the membrane sample had been washed several times in one of the buffers, it was resuspended in the buffer with a final membrane concentration such that the absorbance at 570 nm was about 1.5 in a 1-cm cell. About 300 μL of this suspension was used to fill a small glass vial to the brim. Another 200 μL was used to fill a piece of tygon tubing that had been epoxied closed at one end. The inner diameter of the tygon was such that the tygon tubing fit snugly over the neck of the small glass vial. The filled tygon tubing was squeezed slightly, and then its open end was pushed over the neck of the vial while the squeezing pressure was decreased. The result was a closed, completely filled union of a glass vial with its flexible tygon cap. The optical path length through the vial was 3 mm.

The filled, capped vial, which will hereafter be referred to as the sample, was lowered into the space between two sapphire windows (0.25 in. diameter × 0.125 in. thick), which had been epoxied onto the inside walls of an optical bomb (see Figure 1). The bomb was machined from Berylco 25 (1/2 hard, cold rolled, Beryllium Corp., Reading, PA) and then heat treated at 600 °F for 5 h. Previous experience in our laboratory has shown that such a bomb can be used for pressure work up to 3 kbar and from liquid helium temperatures to over 320 K. The bomb was filled with degassed water, plugged with its indium mushroom plug, attached to the high-pressure generator, and inserted into its thermostating jacket.

The flash photolysis apparatus is shown schematically in Figure 2. The monitoring light was a 100-W tungsten–halogen lamp (OSRAM Halogen-Bellaphot, No. 64625), powered by a Kepco regulated power supply (Model SC-32-15). The light was passed through an interference filter that

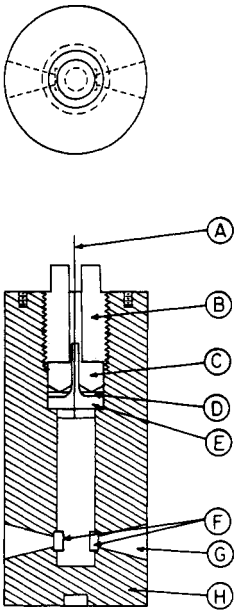

FIGURE 1: Drawings, to scale, showing the main features of the high-pressure optical bomb. The top drawing shows the view along the cylindrical axis. The bottom drawing includes the following details: (A) high-pressure capillary tubing that goes to the pressure generator; (B) bolt; (C) push piece; (D) indium pressure seal; (E) mushroom plug; (F) sapphire windows; (G) light tunnels; (H) Berylco-25 bomb body.

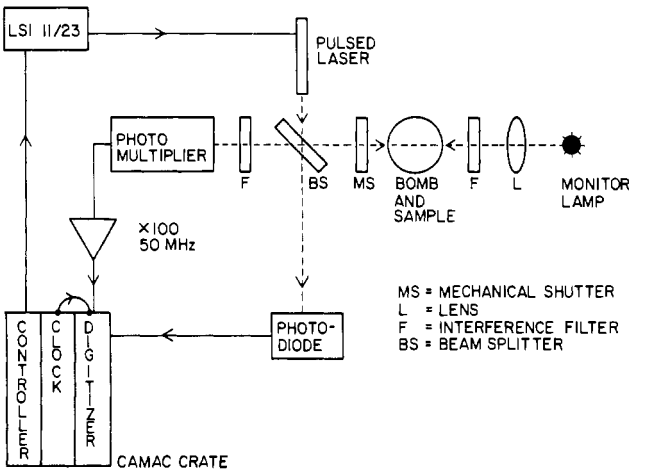

FIGURE 2: Schematic of the flash photolysis apparatus used in the collection of the high-pressure data. Dashed lines show the direction of light from the laser and from the monitoring lamp. Solid lines show the direction of the flow of information and control among electronic components. The mechanical shutter was closed, prior to any measurement, to obtain the value of the signal due to all sources other than light passing through the sample, such as amplifier offset, stray light, dark photocurrent, etc. This artifactual signal was subtracted out of all the data.

was attached, via spring clips, to a thermostated jacket surrounding the bomb. After passing through the sample, the monitoring beam passed through a mechanical shutter and then a combination of cuton or cutoff filters and another interference filter before impinging upon the cathode of an EMI 9816B photomultiplier tube. The high-voltage power supply for the phototube was a Model RE-3010 regulated high-voltage power supply from Northeast Scientific Corp. (Acton, MA). The cathode of the phototube has an S-20 response, and the anode current was kept lower than 3% of the voltage divider current via an appropriate choice of divider network. The photocurrent from the anode was fed directly into a 100× amplifier (Pacific Precision Instruments, Model 2A44 video amplifier, 50-MHz bandwidth). The amplified

signal was sent through a low-pass RC filter with a time constant of 20 ns.

The remainder of the data acquisition system was computer controlled and can be seen in Figure 2. An LSI 11/23 computer was interfaced to the remainder of our apparatus via two pathways: (1) to the pulsed laser via a bit on a parallel I/O card and (2) to the transient recorder via a CAMAC crate and CAMAC crate controller.

First we describe the laser triggering circuit: A subroutine caused one of the bits of the 16-bit word in a parallel I/O board to toggle once. This TTL signal was the input to a high-speed optical isolation chip (HCPL-2601, Hewlett-Packard Corp.), the output of which was used to fire the pulsed dye laser (Phase-R Corp., Model DL-2100C). The dye was Rhodamine 590 dissolved in methanol. The laser pulse was centered at 590 nm, had a pulse width of 400 ns, and had an energy of $\sim$1 J, which was adequate to saturate the absorbance changes.

Next we describe the processing of the analog signal from the video amplifier: The signal was fed into the Analog Input port of a LeCroy 2256A wave form digitizer (LeCroy Research Systems, Palo Alto, CA). The 2256A has a dynamic range of 512 mV and digitizes the input into 8-bit words, which are placed into a circular memory. The 2256A was plugged into one of the slots of the CAMAC crate (Kinetic Systems Corp., Lockport, IL, Model 1510 "minicrate"). The crate was controlled by a Kinetic Systems unibus crate controller (Model 3912). The sampling frequency for the wave form digitizer (hereafter referred to as the TD) was controlled by another programmable module plugged into the crate, a Lecroy 8501 programmable clock.

Our data were collected in cycles of three flashes, with widely differing dwell times for each flash. Each cycle of three flashes is now described in more detail.

Prior to the firing of the laser, the clock was programmed to a fast frequency, so that the TD recorded the filtered video amplifier output with a shortest dwell time, typically 50 ns. The TD has a circular memory of 1024 8-bit words, and it continually records data, with the new data being written over the old data, until it senses the stop trigger. It then records only 896 words, leaving 128 pretrigger words, and stops. The stop trigger circuit contained a photodiode (Motorola Model MRD 500 PIN silicon diode) in a circuit resembling an ECL logic gate. When the laser light intensity into the photodiode exceeded a certain value, the output of the entire stop trigger circuit switched from ground to −800 mV in less than 50 ns, thereby providing the stop trigger edge for the TD.

The first 100 pretrigger words were averaged to calculate the base-line photovoltage of the measurement. (To avoid laser artifact in our base line, we purposely ignored words 101–128.) The photovoltages corresponding to the words in the final 896 channels were divided into the base line, and the logarithms of the quotients were calculated. These calculated absorbance changes were stored in a 896 × 1 array. The program next decreased the clock frequency by a factor of 100 and again fired the laser. Another set of 896 absorbance changes was calculated and placed into another 896 × 1 array. Finally, the clock frequency was decreased by yet another factor of 100, the laser was fired, and a third array was filled with 896 of the slowest data. The filling of these three 896 × 1 arrays with absorbance change data constituted the completion of one data acquisition cycle. Such a cycle typically required about 8 s of real time. In all experiments, we light adapted the sample, repeated the data acquisition cycle 10 times, and averaged the data from the 10 cycles, thereby providing signal/noise improvement in the contents of the three 896 × 1 arrays.

The data in the three 896 × 1 arrays were further averaged and reduced by the following procedure: The user entered into the data acquisition program the number P of final data points desired per decade of time. The computer then divided the data in each 896 × 1 array into $2P$ segments that were equally spaced in log time and averaged all the data points within each such segment. The average time corresponding to this segment was also calculated. The final data set consisted of about $6P \approx 120$ data points, approximately equally spaced in log time from about 0.1 μs to about 1 s. These 120 points thus represent an average of almost 27000 TD samplings, and the slower data in the final data set contain more averaging than the fastest data.

Pressure was applied to the sample by the use of a hydraulic press. A piston in the high-pressure generator (High Pressure Equipment, Inc., Erie, PA) was advanced into a closed, water-filled system that includes the bomb. The bomb was rendered hydraulically continuous with the piston via a stainless steel capillary leading from the high-pressure generator, through the indium plug of the bomb, and into the interior of the bomb. The pressure in the entire closed system was measured with a high-pressure gauge (Model Duragauge, High Pressure Equipment, Inc.) that had previously been calibrated against a Heise gauge (Heise, Inc., Newton, CT).

For each temperature, the kinetics were measured at applied pressures of 0, 0.34, 0.68, 1.02, 1.36, and 1.70 kbar (1 kbar = 10^3 atm = 1.47×10^4 psi). At each pressure, the kinetics were measured by using monitoring wavelengths of 410, 510, and 640 nm. We found that laser artifact in the data persisted for about 500 ns (approximately the duration of the laser pulse) when we monitored at 410 or 510 nm but that such artifact affected our detection system for over 50 μs when we monitored at 640 nm. We were unable to eliminate the artifact at 640 nm and thus always analyzed only the data slower than 80 μs in the 640-nm data sets.

Although no sequential and unbranched first-order model of the photocycle has been completely successful in describing photocycle kinetics (Nagle et al., 1982), we chose for this experiment to model the photocycle kinetics as follows:

$$\frac{d}{dt}\begin{pmatrix}[K]\\[L]\\[M]\\[O]\end{pmatrix} = \begin{pmatrix}-k_{K\to L} & 0 & 0 & 0\\ k_{K\to L} & -k_{L\to M} & 0 & 0\\ 0 & k_{L\to M} & -k_{M\to O} & 0\\ 0 & 0 & k_{M\to O} & -k_{O\to bR}\end{pmatrix}\begin{pmatrix}[K]\\[L]\\[M]\\[O]\end{pmatrix} \quad (3)$$

where [I] denotes the concentration of the intermediate I. We have done this because such a model gives good fits for the faster data (i.e., up to and including the formation of the M intermediate) and because none of the more complicated models gives much better results for the slower part of the photocycle (i.e., the decay of the M intermediate). For the (lower) temperatures at which we are able to resolve two distinct processes much faster than M decay, the fastest rate is K → L and the next fastest is L → M. For the (higher) temperatures at which we could only resolve one process much faster than M decay, that process is L → M. We are confident of these assignments because semilog plots of $k_{K\to L}$ or $k_{L\to M}$ vs. pressure or temperature are smooth.

Data reduction was accomplished by using a variable projection algorithm, which we shall refer to as VARP2. This algorithm (Golub & Pereyra, 1973; Kaufman, 1975) was obtained from Stanford University via Dr. Richard Lozier (Nagle et al., 1982). The input to VARP2 consists of several kinetic data sets that were taken at the same temperature and

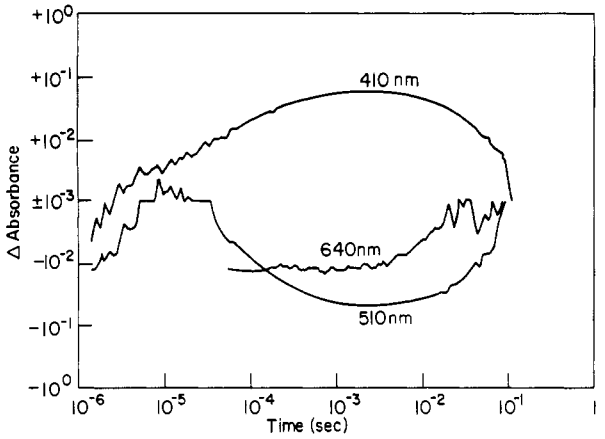

FIGURE 3: Typical data sets collected with the apparatus shown in Figure 2. We show a log–log plot of absorbance change vs. time, with the base line corresponding to $\pm 10^{-3}$, for the three monitoring wavelengths 410, 510, and 640 nm. Data prior to 80 μs at 640 nm are unavailable due to a laser artifact. The data in this figure were taken at a temperature of 9 °C and at atmospheric pressure.

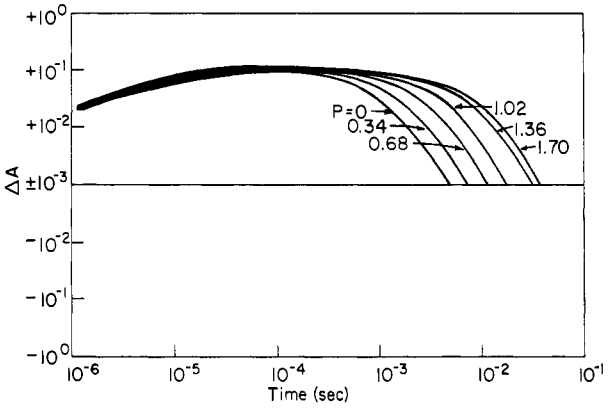

FIGURE 4: Absorbance change as a function of time and pressure, all collected at 410 nm. The pressures are indicated in kilobars. This plot shows the retardation of the photocycle with pressure. The data were taken at 50 °C.

pressure but with different monitoring wavelengths. VARP2 simultaneously fits all the data sets such that (1) each set is the sum of N (user chosen) exponentials *and* (2) the rate constants are the same for all data sets. Only the preexponential amplitudes are different for the different data sets.

Results

Typical data sets are plotted in Figure 3. Note that the plot is log–log, exactly as in our viscosity paper (Beece et al., 1981). Positive absorbance changes of up to 1 = $+10^0$ are plotted above the base line, which is $\pm 10^{-3}$. Negative absorbance changes (i.e., increased light intensity at the photomultiplier as compared with the preflash intensity) are plotted below the base line.

Figure 4 shows the pressure dependence of the kinetics at 410 nm, at T = 50 °C and a variety of pressures. The most obvious qualitative behavior is the retardation of the photocycle with increased pressure.

The retardation is most easily seen as a function of temperature and pressure in Figure 5. In this figure, we have plotted the duration of the photocycle, as measured by the time at which all the absorbance changes have gone to $\pm 10^{-3}$, as a function of both temperature and pressure in a semilog plot. A striking feature of this plot is the saturation effect of pressure on the duration at 1, 9, and 25 °C. The pressure at which saturation occurs is higher for the higher temperatures.

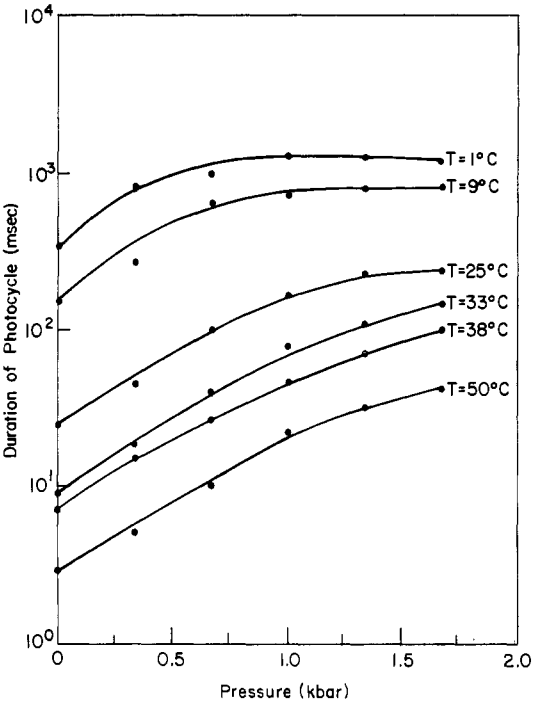

FIGURE 5: Curves showing the duration of the photocycle as a function of temperature and pressure. The curves were drawn near the data points only to guide the eye. The duration of the photocycle was taken to be that time after the laser flash at which all of the 410-, 510-, and 640-nm absorbance change curves had returned to the base-line value of $\pm 10^{-3}$.

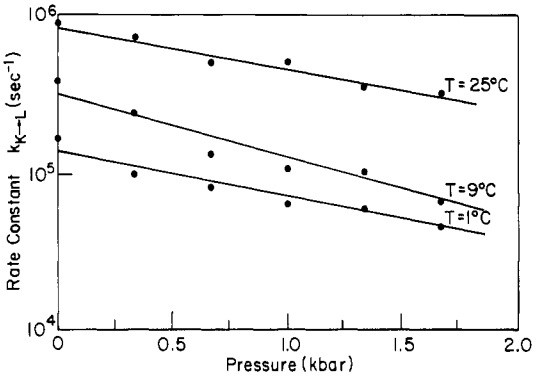

FIGURE 6: K → L rate constant as a function of temperature and pressure. The points were all found by the fitting algorithm VARP2 (see the text and references for details). The curves were drawn near the points only to guide the eye. The data for higher temperatures are not available because of limitations in the speed of our data acquisition system.

The semilog plot in Figure 6 shows the rates for the K → L transition as a function of temperature and pressure. The temperature/pressure compensation ratio, i.e., the temperature increase that offsets the retardation due to a pressure increase, is about 12 °C/kbar. Our laser and detection systems were not fast enough to measure the decay rate for the K intermediate at temperatures higher than 25 °C.

The rates for the L → M transition are shown in Figure 7. The pressure dependence of this rate is less than that of any other step in the photocycle, with the very small $\partial \ln k/\partial P \sim$ −4.4%/0.1 kbar. This rate constant has a temperature/pressure compensation ratio of ~4–5 °C/kbar.

We were unable to fit the post-M data to two or three exponentials with regular temperature and pressure dependence. When we attempted to do so, the pressure dependence of the derived rate constants and preexponential amplitudes was not regular. A parameter that does, however, possess a

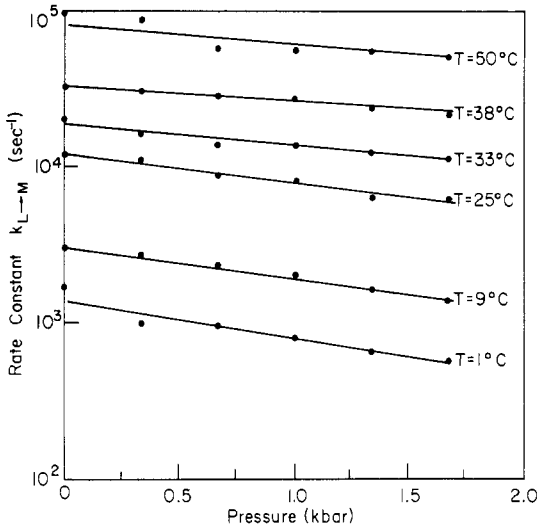

FIGURE 7: L → M rate constant as a function of pressure and temperature. The points were all found by VARP2. The curves were drawn near the points to guide the eye. This figure shows the insensitivity to pressure of the L → M process over a pressure range of almost 2 kbar at temperatures between and including 1 and 50 °C.

regular dependence on pressure and temperature and that describes the slower part of the photocycle (i.e., the part after the formation of M) is the duration of the photocycle, shown in Figure 5. This parameter is essentially unaffected by the fastest processes in the photocycle and is therefore a reflection only of those processes occurring after the formation of M. It is the only regular parameter that we could find to describe the slow data.

The calculated activation enthalpies for K → L were about the same for all the pressures that we measured, so we averaged them together to obtain 53.6 ± 4.6 kJ mol^{-1}. The calculated activation enthalpies for L → M for all the pressures were averaged together to obtain 61.7 ± 2.3 kJ mol^{-1}.

Discussion

An important part of our data analysis is the separation of the effects of temperature and pressure on the solvent and the membrane. In the same way that we had to make isoviscosity plots in our earlier work (Beece et al., 1981) to understand the viscosity effect, we did, a priori, have to make corrections for the pressure and temperature effects on the solvent viscosity in order to discern the pressure effects on the membrane.

In our earlier paper on the effect of solvent viscosity on the photocycle kinetics (Beece et al., 1981), we obtained the following parameters for eq 1: for K to L, $\kappa = 0.25 \pm 0.1$ and $\Delta H^{\ddagger} = 44 \pm 9$ kJ mol^{-1}; for L to M, $\kappa = 0.0 \pm 0.1$ and $\Delta H^{\ddagger} = 66 \pm 13$ kJ mol^{-1}; for M to O, $\kappa = 0.8 \pm 0.2$ and $\Delta H^{\ddagger} = 60 \pm 12$ kJ mol^{-1}; for O to bR, $\kappa = 0.5 \pm 0.2$ and $\Delta H^{\ddagger} = 36 \pm 7$ kJ mol^{-1}. If we take the logarithm of the modified Kramers' relation (eq 1) and differentiate with respect to solvent viscosity, we can calculate the fractional change in the rate due to a unit change in the viscosity. If, in addition, we assume that the activation enthalpies and κ's have no pressure dependence, then we can calculate the expected change in the rate due only to the pressure's modulation of the solvent viscosity. In order to make the analogous calculation for the temperature effect, i.e., in order to understand the contribution of the temperature to the rate constants independent of the viscosity of the solvent, we can take the logarithm of the modified Kramers' relation and then differentiate with respect to temperature. The resulting equation has two terms, one due to the temperature effect on the solvent viscosity and the other due only to an activation enthalpy, as follows:

$$\frac{\partial \ln k}{\partial T} = -\left(\frac{\kappa}{\eta}\right)\left(\frac{\partial \eta}{\partial T}\right) + \frac{\Delta H^{\ddagger}}{k_B T^2} \qquad (4)$$

We have used the water viscosity data of Bridgman (1925) in these calculations. On the basis of his data, we calculated the following expected rate changes due *only* to pressure effects on solvent viscosity: In going from 1 atm to 1 kbar, the K → L rate would *increase* by about 0.5% at 1 and 9 °C and decrease by about 1.5% at 25 °C. Our data show, however, that the measured K → L rate constant decreased by about 80% over the entire temperature range. Similarly, the expected rate changes due only to pressure changes of the solvent viscosity in the L → M transition are nil (because for this transition κ is zero), but we found retardation of that process by a factor of about 40% at the temperatures 1, 9, and 25 °C. Finally, although a pressure-induced solvent viscosity effect on the decay of M would give rise to *increases* of the rate by about 1–2% at 1 and 9 °C and a decrease in the rate by about 4% at 30 °C, we observed about an 80% decrease in the rate of M decay at those temperatures. In the latter calculation, we used a κ of 0.65, which is the average of the values for the M → O and O → bR transitions.

Our conclusion is that the effect on the photocycle kinetics of solvent viscosity changes brought about by pressure is very small compared to the effects of pressure on the membrane. This conclusion obtains for all three processes K → L, L → M, and M → bR, where we have lumped all of the slower processes into the one process M → bR.

Using Bridgman's data again, and also using the above values for the activation enthalpies and κ's, we predict that the temperature modulation of the solvent viscosity should only account for about 9% of the rate change in the K → L process, none of the rate change in the L → M process, and about 17% of the rate change in the M to bR transition. We conclude that the main effect of temperature on the rates for all processes is not via the solvent viscosity.

According to transition-state theory $(\partial \ln k/\partial P) = -\Delta V^{\ddagger}/(k_B T)$, so we can derive values for the activation volumes by plotting log k vs. pressure and calculating the slope. However, we believe that it is extremely unlikely that such apparent activation volumes have any relation to a physical volume when they are calculated for the purple membrane photocycle. Our reasons for doubting the utility of the calculated activation volumes in the case of our purple membrane high-pressure data are as follows: A priori, there is no reason why all of the steps of the photocycle should have positive activation volumes. (Positive activation volumes would be required to give the observed retardation by pressure of *all* of the steps of the photocycle.) Furthermore, even if it were true that all of the activation volumes in the photocycle happened to be positive, it would be a fantastic coincidence that the activation volumes for K → L, L → M, and M decay would be proportional to the respective κ's that we found in our viscosity paper. In fact, proportionality between the apparent $\Delta V^{\ddagger}$ and κ is what we have found: If we take the mean value of the κ's for the M → O and O → bR from our viscosity paper to be the value for κ in "M decay", then the values for κ for the processes K → L, L → M, and M decay are 0.25, 0, and 0.65, respectively. We found in our pressure data that the fractional change f in the rate constants per 0.1 kbar of pressure change ($f = \Delta \ln k/\Delta P$) is approximately −8%, −4%, and −21.5%, respectively, for the three rates. (The latter quantity was obtained by using only pressures up to 0.34 kbar to avoid the saturation effect at high pressure.) The correlation

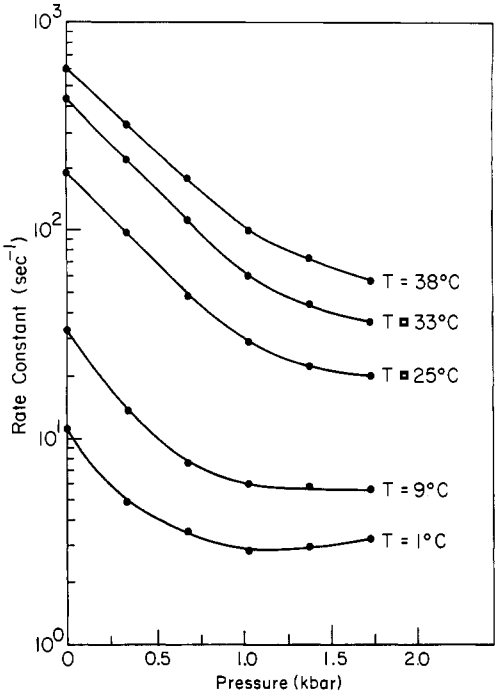

FIGURE 8: Plot of the slowest photocycle rate constant vs. pressure at several temperatures. The rate constants were obtained by using $N = 3$ exponentials in VARP2 for data sets taken at 410 and 510 nm, including all data between 1 μs and 2 s.

coefficient for the linear regression of κ vs. f is −0.98. This value indicates very strong correlation. Therefore, rather than calculating activation volumes for the various stages of the photocycle and then invoking those volumes as the physical "explanation" for the pressure effects on the rates, we believe that the very strong correlation of viscosity effects (measured at atmospheric pressure) and pressure effects points to the modulation of intrinsic membrane viscosity as the primary means by which pressure affects the photocycle kinetics.

It is possible that our difficulties in fitting the slow data to a small number of exponential decays are because the slow processes of the photocycle are simply not first-order processes. In addition, we might also expect ill-behaved parameters even from truly first-order processes if those processes have rate constants that are close together. With the unavoidable noise in the data, fits to a sum of exponentials, where two of the rates are very close to each other, will not necessarily be stable fits; i.e., the parameters found by the fitting algorithm will not necessarily demonstrate smooth pressure and temperature dependence.

A possible complication in the evaluation of the slow data is a reputed phase transition in the lipid in the membrane (Tsuda et al., 1983). Tsuda et al. assert that the critical temperature for this transition is at −42 °C at atmospheric pressure but that the transition can be observed at room temperature by pressurizing the membrane, i.e., that the critical temperature is raised by pressure. They claim that the critical temperature is a linearly increasing function of the applied pressure with a slope of 53 °C/kbar. They base their hypothesis entirely upon a change in the slope of the log k vs. pressure curve at various temperatures, where k refers to one component of their biphasic M-decay data.

When we fit our 410- and 510-nm kinetics to three exponentials using VARP2, so that all of the processes after the formation of M are considered as one process, we also see a shift in the slope of the log k (slowest) vs. pressure curve, particularly at low temperatures (Figure 8). The pressure at which the slope changes, for any given temperature, is in

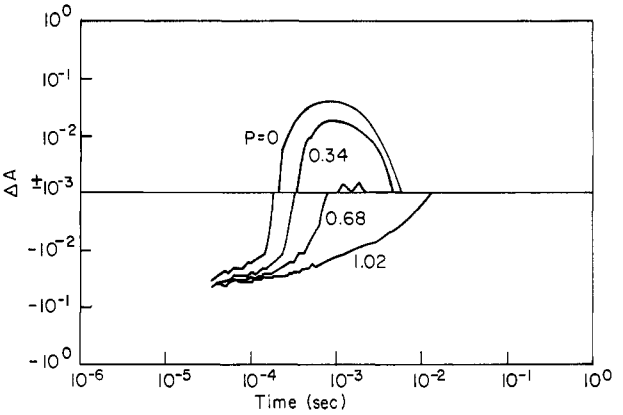

FIGURE 9: Plots of absorbance change as a function of time and pressure. The four curves were all collected at 50 °C by using 640-nm monitoring light, and they show the monotonic decrease in the absorbance change of the sample near the end of the photocycle as the pressure is increased. The pressure is indicated in kilobars.

good agreement with the pressure that Tsuda et al. have reported in their paper. However, we are not at all sure that the data indicate a phase transition. Another possible explanation for their and our data is simply that a "saturation" effect is being observed whereby the membrane has contracted (due to the cold) and has been compressed (by the application of the hydrostatic pressure) to a limiting maximum membrane density.

We have evidence for such an explanation: We have determined the apparent values for the isothermal compressibility and the thermal expansivity of the purple membrane (Marque et al., 1984). Dividing the compressibility by the expansivity gives a $\Delta T/\Delta P = 44$ °C/kbar as the temperature/pressure compensation ratio for which the apparent density of the membrane remains constant. The error on this ratio is large (at least 20%). Furthermore, the intrinsic compressibility of globular proteins is typically larger than the apparent compressibility (Gavish et al., 1983), so that the temperature/pressure compensation ratio that is intrinsic to the membrane is probably larger than 44 °C/kbar. Because of these findings and because of the considerable error in the 53 °C/kbar figure that Tsuda et al. quote, we can conclude that the membrane density is approximately equal at all temperatures at which the log k vs. pressure plot shows a break.

One of the most striking effects of pressure is on the apparent yield of the O intermediate as manifested by the amplitude of the positive ΔA in the 640-nm data sets. Figure 9 shows the apparent suppression of the O intermediate by pressure at 50 °C. Near the end of the photocycle, the positive absorbance change at 640 nm is seen to monotonically decrease with increasing pressure until no positive absorbance change is seen. Similarly, Figure 10 shows the sensitivity of O production to temperature, with higher temperatures giving higher absorbance changes at 640 nm at the end of the photocycle. At 1 and 9 °C, we saw no positive absorbance change at any pressure near the end of the photocycle when we monitored at 640 nm. Our data for the temperature dependence of the O yield are in qualitative agreement with the results of our previous work (Beece et al., 1981).

An attractive hypothesis to explain the pressure and temperature dependence of the O form is as follows: In the O form, a group or set of acidic groups with a substantial negative enthalpy of proton ionization (i.e., ~8 kJ mol^{-1}) is undissociated. Such an un-ionized group would be expected to have the following properties: Pressure would suppress it by shifting the equilibrium to the ionized form. This is because the electrostricted water around charges occupies less volume (i.e.,

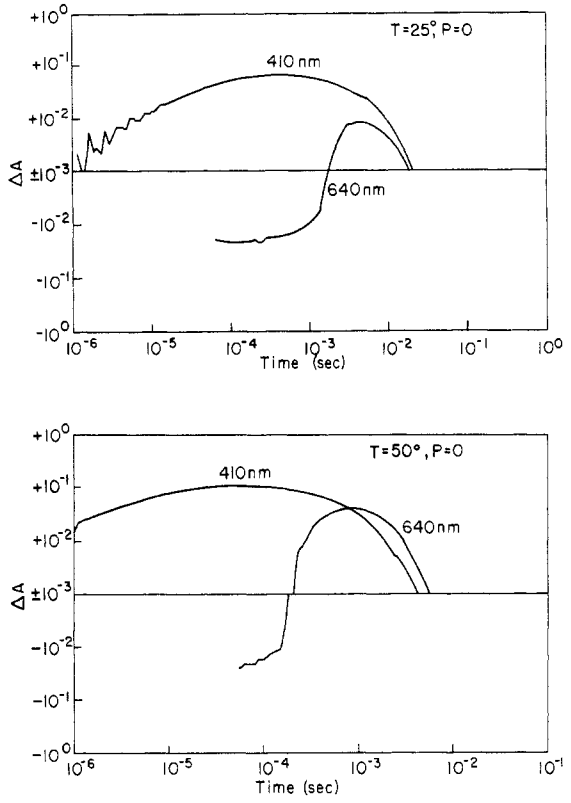

FIGURE 10: Plots of data taken at different temperatures. These plots show the decrease in the positive absorbance signal at 640 nm as the temperature is decreased. Although not shown in this figure, the effect is monotonic from 50 to 9 °C.

is denser) than the bulk water surrounding an undissociated form (Friedman & Krishnan, 1973). LeChatlier's principle requires that pressure shift the equilibrium away from the larger volume species, i.e., away from O.

Higher temperatures would enhance the amount of O via the temperature dependence of the pK if the proton ionization reaction for O proceeds with a substantial negative enthalpy: The direction of the equilibrium will be shifted to the un-ionized form at higher temperatures, i.e., toward O.

By the definition of the equilibrium constant for a proton ionization reaction, the population of the un-ionized species increases as the pH drops, i.e., toward O.

Finally, the presence of salt stabilizes ionized forms by providing screening of the otherwise attracting ions and counterions. We would therefore expect the presence of salt to decrease the concentration of the O intermediate.

In fact, there already are published data that show that O formation is suppressed at low temperature (Beece et al., 1981; Nagle et al., 1982), high pH (Ort & Parson, 1978), and high salt (Sherman et al., 1976). The pressure data described in this paper (see especially Figure 9) show that the O form is apparently suppressed by pressure. To summarize, the pH, temperature, pressure, and salt effects all support the above-formulated hypothesis concerning the nature of the O intermediate.

One is tempted to jump to the conclusion that a carboxylic acid group on one or more of the residues of bacteriorhodopsin (e.g., glutamic acid and/or aspartic acid) is responsible for the O form, i.e., that such a group becomes protonated during the time we detect O. Such a hypothesis is immediately compatible with the observed pH and pressure effects. However, the published salt effect is not especially compelling (Sherman et al., 1976). It was found that high concentrations of NaCl (3 M) inhibited O production, whereas the presence of KCl (up to saturation) had no effect on O production. In addition, the above-mentioned hypothesis is not, a priori, compatible with the observed temperature effect. The enthalpies of proton ionization of the residues of glutamic acid and aspartic acid are close to zero. We would therefore expect no dependence of the proton ionization equilibrium on temperature. We point out, however, that the enthalpy of ionization for ionizable groups may be very different in the interior of a protein (particularly a hydrophobic protein like bacteriorhodopsin) as compared with its value in a simple aqueous solution (Tanford, 1962).

We will now discuss some of the consequences of our "O hypothesis", i.e., the idea that some acidic group (or groups) is undissociated in the O form. A priori, the most important consequence of this hypothesis is the incompleteness of the first-order differential equations that we have used to describe the photocycle (eq 3). The rate of O formation should be proportional to the hydrogen ion concentration in addition to the concentration of the M form. Because the location of the proton binding site may be deep within the protein, the proportionality might not be direct but might instead be to some small positive power of the hydrogen ion concentration (much as we have modified the Kramers' relation, with a nonunity power of the viscosity, to represent the shielding of the reaction site from the solvent by the protein). The important qualitative and testable prediction that can be made on the basis of our hypothesis is that, at a given temperature and pressure, the formation of O will accelerate as the pH is decreased.

In fact, such an experiment was performed by Ort & Parson (1978). They found that the rate constant for the formation of the O intermediate at atmospheric pressure increased by a factor of about 3 when the pH was lowered from 8.0 to 6.0, a finding that supports our O-intermediate hypothesis.

Finally, we wish to consider another approach to analyzing the effect of membrane viscosity on the various processes of the photocycle. We make the following, admittedly crude, assumptions and approximations: (1) The apparent density, expansivity, and isothermal compressibility of the purple membrane (Marque et al., 1984) are equal to the intrinsic density, expansivity, and isothermal compressibility of purple membrane. This assumption is equivalent to saying that the contribution of bound water to these apparent quantities is zero. (2) Purple membrane shares the property of nonassociated liquids (e.g., n-hexane), that its viscosity is determined essentially by its density and that temperature and pressure effects on the viscosity of the membrane are byproducts of their effects on the density (Hildebrand, 1979).

With these assumptions and approximations, consider the measured rate constant, at a temperature T_1 and pressure P_1, for any process of the photocycle, say L → M. Now consider the rate constant at $T_2 = T_1 + 44$ °C and $P_2 = P_1 + 1$ kbar. At this new temperature and pressure, the viscosity of the membrane is the same as at (T_1, P_1), because the temperature/pressure compensation ratio for constant membrane density is 44 °C/kbar. Suppose the rate at (T_2, P_2) is the same as the rate at (T_1, P_1). This would suggest that the kinetics are strongly influenced by the membrane viscosity and not by an activation barrier. Such a conclusion would be very strongly supported if the same result obtained for an arbitrary choice of (T_1, P_1). If, however, the rate at (T_2, P_2) is larger than at (T_1, P_1) (i.e., if the $\Delta T/\Delta P$ compensation ratio for the rate is less than 44 °C/kbar), then we can invoke the existence of an activation enthalpy to account for the difference in the rates. A slight difference in the rates between (T_1, P_1) and (T_2, P_2) suggests a small activation enthalpy, and a large difference

suggests that there is a large activation enthalpy.

If we now actually look at the measured temperature/pressure compensation ratios for constant rates and compare those ratios with 44 °C/kbar, we observe the following: The temperature/pressure compensation ratios for the K → L and L → M processes are approximately only 25% and 10%, respectively, of the ratio for constant membrane density. This suggests that the largest effect of temperature on these rate constants is via the activation enthalpy, not via the membrane density. However, the combined processes denoted as M → bR show a $\Delta T/\Delta P$ ratio closer to 50% of the ratio for constant membrane density. The calculation suggests that much of the temperature effect, therefore, for this particular process is due to the change in the membrane viscosity with temperature and is not due entirely to the activation barrier.

It would not be useful to carefully quantify the above calculations because the assumptions upon which they are based are not strictly correct. In particular, the apparent temperature/pressure compensation ratio is probably smaller than the intrinsic ratio for constant membrane density. In addition, purple membrane is clearly not a homogeneous nonassociated fluid, so the correlation between density and viscosity in purple membrane is probably not as tight as it has been shown to be in nonassociated liquids (Hildebrand, 1979). What *is* important in the calculation above is the conceptual approach in which a highly modified Kramers' theory is used to consider the effects of pressure and temperature on the bulk properties of the membrane and not just on the local "reactive site" in the protein. Vis-à-vis our solvent viscosity paper (Beece et al., 1981), the above calculations suggest that our reported values for the activation enthalpy for the K → L and L → M processes are probably quite accurate but that the values that we reported for the enthalpies of the latter steps in the photocycle may be considerably too large.

At this point, it is important to point out that there is experimental evidence which suggests strongly that, for some membrane-bound proteins, the viscosity of the membrane plays the central role in the kinetics of the protein. Chong (1982) showed that the kinetics of $(Na^+ + K^+)$ATPase in its native membrane were independent of temperature and pressure as long as the fluidity of the membrane was kept constant. Unlike our work, where we have *assumed* a strong correlation between apparent membrane density and intrinsic membrane viscosity, Chong *measured* the depolarization of fluorescence in his membranes and defined fluidity in terms of the depolarization. We point out that the interpretation of fluidity from depolarization experiments is not straightforward and is, in fact, controversial. The important point to be learned from Chong's work is that our temperature/pressure compensation calculations have been motivated by his experimental results in the kinetics of another membrane-bound protein.

Acknowledgments

We thank Professor Thomas G. Ebrey and Dr. Rajni Govindjee for supplying us with purple membrane samples. We also thank Dr. Richard Lozier for the source code to VARP2 and Dr. Daniel Beece for modifying them for our use. We thank Bruce Mather for writing the source code that we used for data acquisition and plotting. Professor Benjamin Gavish, of the Hebrew University in Jerusalem, provided much of the stimulus to interpret our results in terms of membrane fluidity. Professors Gregorio Weber and Harry Drickamer generously shared their knowledge and experience concerning the building of high-pressure apparatus. We also thank Dr. Christopher Hardy for his design from which our optical bomb design was derived. We also gratefully acknowledge the efforts of Gavin Dollinger in assembling and debugging the laser, Joe Vittitow in the debugging of the flash photolysis system, Jeffrey Ziegler in the design of the trigger circuits, and Mi-Kyung Hong in their construction.

References

Beece, D., Eisenstein, L., Frauenfelder, H., Good, D., Marden, M. C., Reinisch, L., Reynolds, A. H., Sorensen, L., & Yue, K. T. (1980) *Biochemistry 19*, 5147.

Beece, D., Bowne, S. F., Czege, J., Eisenstein, L., Frauenfelder, H., Good, D., Marden, M. C., Marque, J., Ormos, P., Reinisch, L., & Yue, K. T. (1981) *Photochem. Photobiol. 33*, 517.

Birge, R. R. (1981) *Annu. Rev. Biophys. Bioeng. 10*, 315.

Bridgman, P. W. (1925) *Proc. Natl. Acad. Sci. U.S.A. 11*, 603.

Chin, J. H., Trudell, J. R., & Cohen, E. N. (1976) *Life Sci. 18*, 489.

Chong, P. L.-G. (1982) Ph.D. Dissertation, Department of Biochemistry, University of Illinois at Urbana-Champaign.

Chong, P. L.-G., & Cossins, A. R. (1983) *Biochemistry 22*, 409.

Cossins, A. R., & Prosser, C. L. (1982) *Biochim. Biophys. Acta 687*, 303.

Cossins, A. R., Kent, J., & Prosser, C. L. (1980) *Biochim. Biophys. Acta 599*, 315.

Friedman, H. L., & Krishnan, C. V. (1973) *Water: A Comprehensive Treatise* (Franks, F., Ed.) Vol. 3, Plenum Press, New York.

Gavish, B., Gratton, E., & Hardy, C. J. (1983) *Proc. Natl. Acad. Sci. U.S.A. 80*, 750.

Golub, G. H., & Pereyra, V. (1973) *SIAM J. Numer. Anal. 10*, 413.

Govindjee, R., Ebrey, T. G., & Crofts, A. R. (1980) *Biophys. J. 30*, 231.

Henderson, R. (1977) *Annu. Rev. Biophys. Bioeng. 6*, 87.

Hildebrand, J. H. (1979) *Viscosity and Diffusivity: A Predictive Treatment*, Wiley, New York.

Kaufman, L. (1975) *Bit 15*, 49.

Kramers, H. A. (1940) *Physica (Amsterdam) 7*, 284.

Lozier, R. H., Bogomolni, R. A., & Stoeckenius, W. (1975) *Biophys. J. 15*, 955.

Marque, J., Eisenstein, L., Gratton, E., Sturtevant, J. M., & Hardy, C. J. (1984) *Biophys. J.* (in press).

Nagle, J. F., Parodi, L. A., & Lozier, R. H. (1982) *Biophys. J. 38*, 161.

Ort, D. R., & Parson, W. W. (1978) *J. Biol. Chem. 253*, 6158.

Ottolenghi, M. (1980) *Adv. Photochem. 12*, 97.

Sherman, W. V., Slifkin, M. A., & Caplan, S. R. (1976) *Biochim. Biophys. Acta 423*, 238.

Stoeckenius, W., & Bogomolni, R. A. (1982) *Annu. Rev. Biochem. 51*, 587.

Stoeckenius, W., Lozier, R. H., & Bogomolni, R. A. (1979) *Biochim. Biophys. Acta 505*, 215.

Tanford, C. (1962) *Adv. Protein Chem. 17*, 69.

Tsuda, M., Shirotani, I., Minomura, S., & Terayama, Y. (1976) *Bull. Chem. Soc. Jpn. 49*, 2952.

Tsuda, M., Govindjee, R., & Ebrey, T. G. (1983) *Biophys. J. 44*, 249.